Research on Lubrication Characteristics of Harmonic Gear Transmission Meshing Area

Xiangyang Xu[1,*], Xupeng Fan[1], Peitang Wei[2], Baojun Yang[3]

1. School of Mechatronics and Vehicle Engineering, Chongqing Jiaotong University, ChongQing, 400074, China
2. College of Mechanical Engineering, Chongqing University, Chongqing 400044, China
3. Chongqing Huashu Robot Co., Ltd., Chongqing 400714, China

In order to analyze the lubrication characteristics of harmonic gears and lay the foundation for the study of its gear tooth failure performance and dynamic characteristics, based on the tooth contact geometry of harmonic gear, the integrated curvature radius, tooth load, and entrainment velocity at the *meshing point of the gear teeth in the harmonic gear transmission are analyzed. A finite-length linear contact elastohydrodynamic lubrication (EHL) model for harmonic gears is established. The numerical calculation method is used to solve the oil film thickness and pressure distribution in the lubricating area, and the effects of rotational speed and temperature on the contacting load ratio and film thickness ratio of the meshing area are studied, as well as the change of oil film stiffness under different working conditions. The results show that along the meshing direction, the pressure is small at the end and reaches a peak at the center, and the film thickness is the largest in the entrance area and is evenly distributed in the center contact area. As the speed increases, the gear tooth contact load ratio decreases, the oil film thickness ratio increases, the stiffness of the oil film decreases significantly, and the lubrication effect is improved; but the temperature has the opposite effect. Proper increase of rotation speed and decrease of oil temperature can effectively improve the lubrication characteristics of the system.*

Key words: harmonic gear transmission; elastohydrodynamic lubrication; meshing area; lubrication characteristics

Highlights*:*
- The integrated curvature radius, the entrainment velocity and the load at the meshing point of harmonic gear are analyzed and extracted for the harmonic gear lubrication.
- A finite line contact elastohydrodynamic lubrication model for harmonic gears is established.
- The complex iterative method is used to solve the lubrication equation to obtain high precision.
- The lubrication characteristics and the change of oil film stiffness under different working conditions are explored.

0 INTRODUCTION

Harmonic gear transmission is a new type

---

of transmission mode，which is different from traditional gear transmission. It mainly transfers power through the deformation of flexible gears, with small volume, high precision, large transmission ratio and other excellent performance. Therefore, it is widely used in the field of high-precision machinery such as industrial robots, aerospace equipment and so on [1-2]. However, there are nonlinear stiffness, hysteresis and friction nonlinear factors in harmonic gear drive, which restrict the improvement of the accuracy and efficiency of harmonic gear drive. And the interaction between lubrication oil and gears will affect the power loss of gears and transmission accuracy [3-4]. So it is necessary to study the lubrication performance of gear system for improving its efficiency and accuracy. Therefore, the analysis of the geometry and motion parameters of harmonic gear teeth and the research of harmonic gear lubrication control can promote the analysis of the friction and failure mechanism of harmonic gear transmission and improve the nonlinear behavior of the system.

Gorla et al. [5-6]used an improved CFD simulation method to predicting the power loss caused by the interaction between gears and lubricant, simulated the wind resistance, agitation and cavitation by a comprehensive time-saving numerical simulation method, and compared the experimental data with the numerical simulation results in terms of power loss and lubricant distribution with good agreement.

In the study of elastohydrodynamic lubrication, at the beginning, various numerical solutions were mainly aimed at infinite line contact and point contact problems, but in fact, in engineering practice, most lubrication problems are finite line contact problems. In the static contact elasticity theory [7], the contact pressure

distribution of the finite line contact pair with straight generatrix profile is different from that of the classical Hertz infinite line contact theory, and there will be "edge effect" at the end part. And the contact width of the gear is limited, so the infinite line contact model cannot simulate the actual situation of the end part well. Scholars have carried out some researches on the problem of finite-line wire contact elastohydrodynamic lubrication. Wymer [8] studied the elastohydrodynamic lubrication of tapered roller by means of optical interference method, and obvious edge effect was observed at the end. Park [9] established the elastohydrodynamic lubrication model of finite length line contact, and found that in the middle of the roller, the pressure distribution is almost the same as that of the infinite line contact. However, near the end part, the results of EHL are quite different from that of infinite solution, where the pressure reaches its peak. Zhu et al. [10] established a finite length EHL model for helical gears and found that the second pressure peak occurred at the end part.

Wei et al. [11] established a mixed lubrication model for cycloidal pinwheels, and discussed the effects of contact load and radius of curvature on lubrication conditions. Liu et al. [12] developed a line contact model of thermoelastic hydrodynamic lubrication under the condition of ultrathin film, and studied the influence of speed and dynamic load on the lubrication performance of a spur gear pair. Ouyang et al. [13] established an integrated friction dynamic lubrication model of spur gear pairs considering dynamic load and elastohydrodynamic lubrication, and analyzed the relationship between the dynamic model and the elastohydrodynamic lubrication model through an iterative algorithm. Xiao et al. [14] discussed the distribution of central pressure and film thickness

in the lubrication area before and after considering the thermal effect, and analyzed the influence of heat on the film damping, and the influence of contact force, speed and number of teeth on the film damping. Sikorski [15] et al. added graphite and molybdenum disulfide into the lubricant, and through the experimental verification of the two kinds of ball bearings, measured the power of the internal friction of the ball bearings under the action of both at low temperature with the change of temperature, and found that the two additives can effectively improve the lubrication performance. Scaraggi et al. [16] analyzed the lubrication of pin-pulley interface in CVT of gear chain industrial chain, and found that the lubrication mode at the interface was determined by a series of hydrodynamic and hybrid lubrication stages. Ciulli et al. [17] presents a model for predicting scuffing considering various lubrication states during the operation of the machine, and the effectiveness of the model is verified through experiments. Li et al. [18] used the elastohydrodynamic lubrication (EHL) method to calculate oil film thickness and pressure distribution in predicting roller bearings' skidding for obtaining more accurate oil film resistance. Li et al. [19] carried out a life test on the space harmonic reducer, finding that the flexspline and bearings would wear under the condition of separate grease lubrication, and analyzed the effects of different factors such as load and temperature on lubrication. Li et al. [20] aimed at the calculation of the stiffness of the elastohydrodynamic oil film in the point contact area, established an oil film stiffness calculation model, and verified the accuracy of the model through experiments.

However, at present, few scholars have quantitatively analyzed the influence of working conditions on the lubrication characteristics and oil film stiffness of gear meshing areas based on tooth contact geometry. Therefore, the entrainment velocity, the integrated curvature radius and the load distribution in the meshing area of harmonic gears are analyzed. Then, the elastohydrodynamic lubrication model of harmonic gear transmission based on the finite line contact is established. And the numerical method is used to solve the lubrication area. The lubrication characteristics and the oil film stiffness in meshing area are quantitatively analyzed with the change of rotational speed and oil temperature.

1 METHODS

The elastic deformation equation, lubricant viscosity equation and density equation are functions of pressure, which are solved by the compound iterative method after being combined with the Reynolds equation. The specific steps are as follows:

Firstly, the basic parameters, initial pressure and initial geometric film thickness are input, and the initial elastic deformation is obtained by integral solution, and the initial film thickness is obtained by substituting the obtained results into the film thickness formula. Secondly, the initial film thickness is substituted into Reynolds equation, and all the nodal pressures can be obtained. Then, the elastic deformation and film thickness are recalculated by the obtained pressure, and the iterative process is repeated using the above calculation results as the input of the next iteration until the convergence solution with accuracy better than 10^{-4} is obtained.

2 EXPERIMENTAL

2.1 Principle of harmonic gear transmission

As shown in Fig. 1, the harmonic gear transmission system is mainly composed of a wave generator, a flexspline and a circular spline. Before assembly, the original profile of the flexspline is circular, and the circular pitch of the flexspline is the same as that of the circular spline, but the number of teeth of the flexspline is slightly less than that of the circular spline, while the maximum diameter of the wave generator is slightly larger than that of the inner circle of the flexspline. When the wave generator is installed in the flexspline, the deformation of the flexspline is forced, and the initial deformation force is generated. So the power is transmitted through the meshing in and out of deformation of the flexspline as a flexible component. And the lubrication characteristics of flexspline and circular spline in the conjugate meshing area the main research target in the next step.
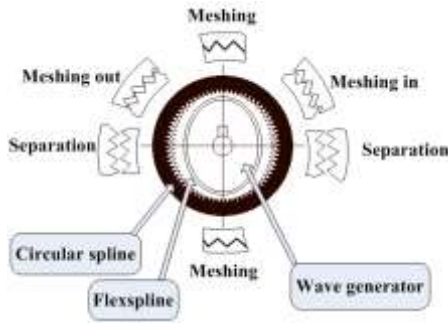

Fig. 1 *Schematic diagram of harmonic gear drive*

The basic parameters of harmonic gear transmission are shown in Table 1.

Table 1. *Basic parameters of harmonic gear transmission*

Parameters	Value
Number of flexspline	200
Number of circular spline z	202
Modulus [mm]	0.5
Tooth width [mm]	12
Transmission ratio	100
Pressure angle	20°
Rated speed of wave generator [rpm]	3000
Output torque [N·m]	400
Circular spline material density [kg/m³]	7.84×10^3
Elastic modulus of circular spline E_2 [Pa]	2.06×10^{11}
Poisson's ratio of circular spline material v_2	0.3
Material density [kg/m³]	7.83×10^3
Elastic modulus of flexspline E_1 [Pa]	2.01×10^{11}
Poisson's ratio of flexspline material v_1	0.3
Surface roughness of flexspline [μm]	0.34
Surface roughness of circular spline [μm]	0.35

2.2 Establishment of Elastohydrodynamic Lubrication Model

2.2.1 *Geometric and kinematic analysis*

For the convenience of discussion of lubrication characteristics between flexspline and circular spline in the conjugate meshing area, as shown in Fig. 2, in the harmonic gear transmission, the meshing of the flexible and the circular spline be approximated as two finite-length cylindrical rollers contacting each other, where x is the direction of motion, and R_{k1}、 R_{k2} are the curvature radii of meshing point of the flexspline and the circular spline, respectively.
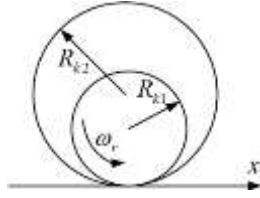
Fig. 2 *Finite-length line contact model*

The following Fig. 3 shows the transmission relationship during meshing. R and G are the tooth curves of the flexspline and the circular spline, k is the meshing point, O_{b1} and O_{b2} are the corresponding base circle centers of the flexspline and the circular spline, respectively, r_{b1} and r_{b2} are the the base circle radii of the meshing point k on the flexspline and the circular spline, and T is the common normal line of the two base circles, and the meshing point k is on the common normal line T.
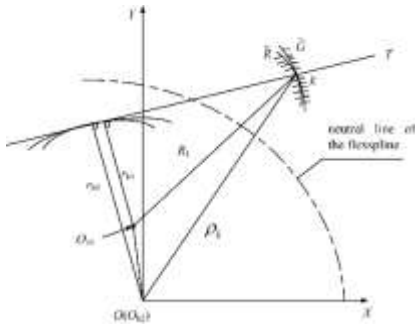

Fig. 3 *Schematic diagram of the transmission relationship of the meshing point*

According to the above transmission relationship diagram, it can be concluded that when the gear teeth of the harmonic reducer mesh, the curvature radii of the meshing points of the flexspline and the circular spline are shown as follows:

$$R_{k1} = \sqrt{R_1^2 - r_{b1}^2} \ , \ R_{k2} = \sqrt{\rho_k^2 - r_{b2}^2} \qquad (1)$$

where, R_1 is the distance from the center of the flexspline base circle to the meshing point, and

ρ_k is the polar radius of the meshing point k.

Then the comprehensive curvature radius R at the meshing point required for the lubrication calculation is obtained by the following Eq. (2):

$$R = \frac{R_{k1} \cdot R_{k2}}{R_{k2} - R_{k1}} \qquad (2)$$

Fig. 4 is a schematic diagram of the velocity at the meshing point k during the movement of the teeth of the flexspline. Where, ω represents the angular velocity; C represents the intersection of the line between the coordinate origin and the meshing point and the neutral line of the flexspline. V_{ek}、V_{rk}、V_{tk} are the velocity of the involved motion, the radial and circumferential elastic deformation, respectively.
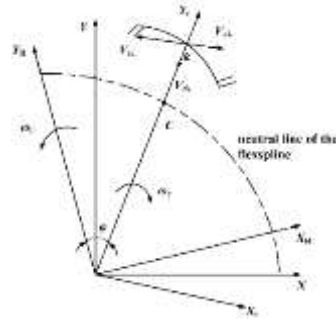

Fig. 4 *Schematic diagram of meshing point speed*

Given that the angular velocity of the wave generator is ω_H and the angular velocity of the flexspline is ω_r. The relative motion velocity of the k-point is the combined velocity of the implication velocity (V_{ek}) and elastic deformation velocity (V_{rk}, V_{tk}), which can be shown by the following Eq. (3):

$$\vec{V}_K = \vec{V}_{ek} + \vec{V}_{rk} + \vec{V}_{tk} \qquad (3)$$

Then the required meshing point entrainment velocity u in the lubrication equation is the component of the resultant velocity along the tangential direction of the tooth profile.

In the meshing direction, the variation of

comprehensive curvature radius R and the entrainment speed u at each meshing position are shown in Figure 5 below:
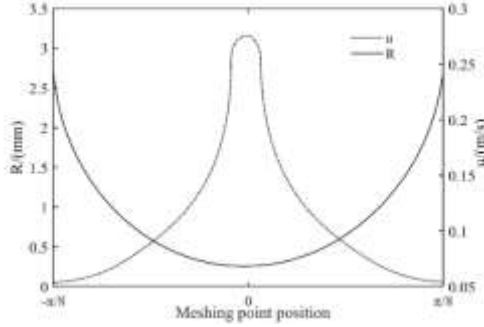

Fig. 5 The *variation of comprehensive curvature radius R and entrainment speed u*

Different from ordinary gear load distribution, the load distribution between the teeth of harmonic gear drive is complex in theoretical calculation, especially when considering the effect of lubricating oil film. Therefore, on the basis of summarizing experimental data results when there is no lubrication, it is found that the distribution law is similar to the cosine distribution shown in the figure below.
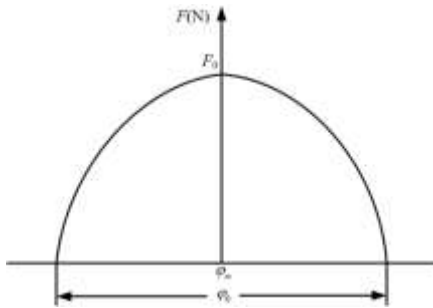

Fig. 6 *Simplified curve of load distribution*

Therefore, the tooth load F can be expressed by

$$F = F_0 \cos \frac{\pi(\varphi - \varphi_m)}{\varphi_0} \qquad (4\text{-}1)$$

where, F_0 is the maximum load, φ is the position

of meshing point, φ_m is the position of the maximum load, φ_0 is the size of the actual meshing area. Generally, $\varphi_m = 0$ and $\varphi_0 = \pi/4$. The above formula is simplified to

$$F = F_0 \cos 4\varphi \qquad (4\text{-}2)$$

The maximum load F_0 can be obtained from the applied external load, that is, the torque T_{in} as follows:

$$F_0 = \frac{T_{in}}{r_{b2} \cdot \sum_{i=-N}^{N} \cos\left(i \cdot \frac{8\pi}{z}\right)} \qquad (4\text{-}3)$$

where, z is the number of the circular spline teeth, and N is the parameter of the number of meshing teeth (N=[z/10]).

2.2.2 Establishment of lubrication model

Using Newtonian fluid as lubricant, the Reynolds equation of lubrication control in the meshing area of harmonic gear transmission is shown as follows:

$$\frac{\partial}{\partial x}\left(\frac{\rho}{12\eta}h^3\frac{\partial p}{\partial x}\right) + \frac{\partial}{\partial y}\left(\frac{\rho}{12\eta}h^3\frac{\partial p}{\partial y}\right) = u\frac{\partial(\rho h)}{\partial x} + \frac{\partial(\rho h)}{\partial t}$$

$$(5\text{-}1)$$

where, p is the oil film pressure; h is the oil film thickness; u is the entrainment velocity, ρ is the lubricant density, η is the lubricant viscosity, respectively.

The boundary conditions of Reynolds equation are:

$$\begin{cases} p(x_{in}, y) = p(x_{out}, y) = p(x,0) = p(x, y_l) = 0 \\ \partial p(x_{out}, y)/\partial x = 0 \end{cases}$$

$$(5\text{-}2)$$

where x_{in} and x_{out} are the boundary of calculation area and y_l is the position of gear end face.

The composition of the oil film thickness is shown in Fig. 7 and is composed of the central film thickness h_0, the geometric film thickness $x^2/2R$, the surface roughness $\mu(x, y)$, and the comprehensive elastic deformation $\delta(x, y)$.
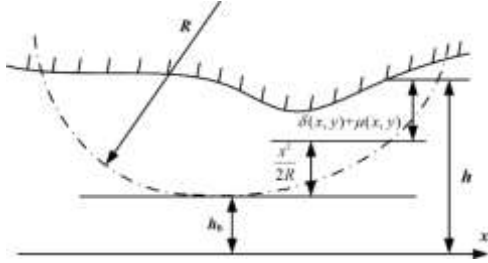

Fig. 7 *Schematic diagram of film thickness*

According to the above Fig. 7, the film thickness formula can be obtained as:

$$h = h_0 + \frac{x^2}{2R} + \mu(x, y) + \delta(x, y) \qquad (5\text{-}3)$$

Where the comprehensive elastic deformation $\delta(x, y)$ can be expressed as:

$$\delta(x, y) = \frac{2}{\pi E} \iint_\Omega \frac{p(s,t)}{\sqrt{(x-s)^2 + (y-t)^2}} ds dt \quad (5\text{-}4)$$

where E is the comprehensive elastic modulus and Ω is the calculation domain.

The equivalent elastic modulus is calculated by the following Eq. (5-5):

$$\frac{2}{E} = (1 - v_1^2)/E_1 + (1 - v_2^2)/E_2 \qquad (5\text{-}5)$$

where, E_1, E_2, v_1, v_2 are the elastic moduli and Poisson's ratios of the flexspline and the circular spline materials, respectively.

The viscosity and density equations are expressed as:

$$\eta = \eta_0 \exp\left[\left(\ln \eta_0 + 9.67\right)\left(1 + 5.1 \times 10^{-9} p\right)^z \left(\frac{T_1 - 138}{T_0 - 138}\right)^{-s} - 1 \right]$$

$$(5\text{-}6)$$

$$\rho = \rho_0 \left(1 + \frac{0.6 \times 10^{-9} p}{1 + 1.7 \times 10^{-9} p}\right) - 0.7 \times 10^{-3}\left(T_1 - T_0\right)$$

$$(5\text{-}7)$$

where, T_1 is the lubricant temperature, T_0 is the ambient temperature, η_0 is environmental viscosity, ρ_0 is the environmental density,

$$z = \frac{\alpha}{5.1 \times 10^{-9}\left(\ln \eta_0 + 9.67\right)} \,,\, s = \frac{\beta\left(T_0 - 138\right)}{\ln \eta_0 + 9.67} \,,\, \alpha$$

is the viscosity pressure coefficient and β is the viscosity temperature coefficient, respectively.

The basic initial parameters of the lubricant are shown in Table 2 below:

Table 2 *Lubricant parameters*

Parameters	Value
Ambient temperature T_0 [K]	313
Ambient viscosity η_0 [Pa·s]	0.04
Ambient density ρ_0 [kg/m³]	870
Viscosity pressure coefficient α [m²/N]	2.2×10⁻⁸
Viscosity temperature coefficient β [K⁻¹]	0.0476

The equilibrium equation of the contact area pressure and external load is:

$$F = \iint_\Omega p\left(x, y\right) dx dy \qquad (6)$$

2.2.3 Oil film stiffness

For the oil film stiffness, this paper uses the average film thickness method to calculate, as shown in formula (7).

$$k_{\text{oil}} = \frac{\Delta f}{\Delta \overline{h}} \qquad (7)$$

where, Δf is the load increase of the oil film, and $\Delta \overline{h}$ is the average oil film thickness increase from the entrance area to the exit area.

$$\Delta \overline{h} = \sum_{i=n1}^{n2} \frac{h_i(f)}{(n_2 - n_1)} - \sum_{i=n1}^{n2} \frac{h_i(f + \Delta f)}{(n_2 - n_1)} \qquad (8)$$

where, n_1 and n_2 are the nodes where the pressure in the inlet area is generated and the pressure in the outlet area disappears. And the number of nodes in x and y directions is 129 × 129.

3. RESULTS

According to the elastohydrodynamic lubrication control equation, the pressure distribution and oil film thickness in the meshing area of harmonic gear are obtained by numerical calculation method, and the influence of rotation speed and oil temperature conditions on the lubrication performance parameters such as contact load ratio, film thickness ratio and oil film stiffness of harmonic gear is analyzed.

3.1 Pressure and oil film distribution

First, the numerical method is used to calculate the numerical solution of the elastohydrodynamic lubrication of the harmonic gear transmission. The oil film thickness and pressure distribution between the contact interfaces are shown in Fig. 8 below.
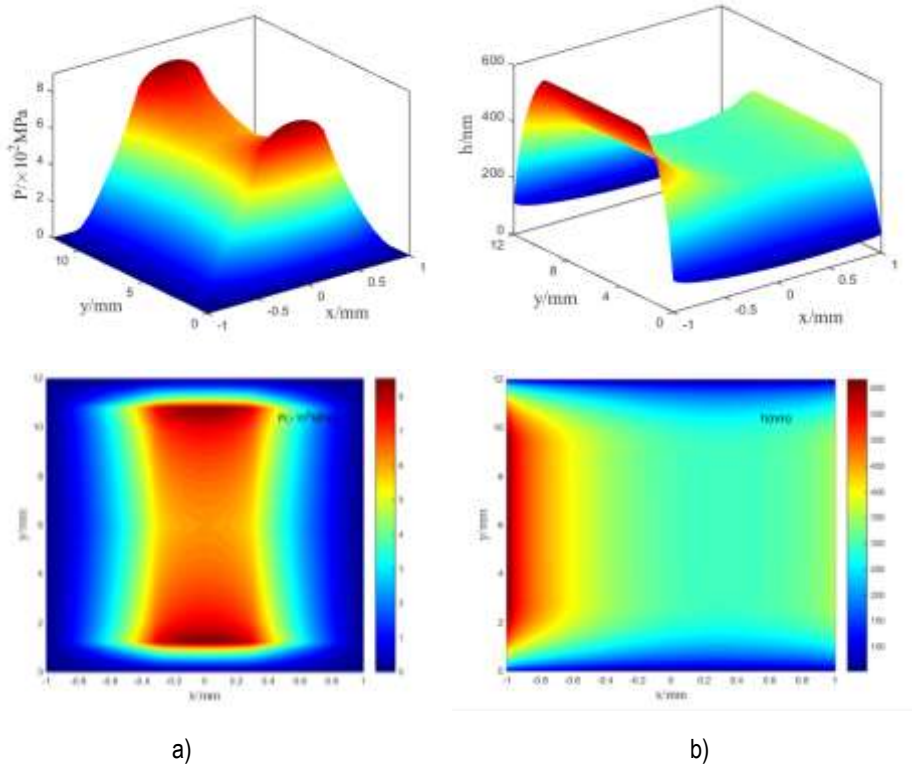
a)   b)

Fig. 8 *Numerical solution of pressure and film thickness in the meshing area; (a) pressure distribution, and (b)oil film thickness distribution*

It can be seen that the pressure at both ends in the axial Y direction is significantly higher than that in the middle, resulting in an end leakage effect. While in the X direction, the pressure is greater as it approaches the center of the meshing point and the pressure peaks at X = 0, indicating that the pressure along the meshing line is the largest at the center of meshing. The oil film thickness reaches its peak in the entrance area in the X direction, and

Xu, X. - Fan X. – Wei P. – Yang B.

the distribution is flat in the contact area. The oil film at both ends in the Y direction is smaller than the middle part, producing an end effect. This is because the main difference between the finite line contact and the infinite line contact is the end leakage effect, which makes the pressure at both ends higher than the middle part, while the film thickness trend is the opposite. The relevant research results have been introduced in another paper of the author [10], and similar phenomena have been found in other scholars' literature [8-9].

3.2 Influence of working condition on lubrication characteristics of contact area

In order to study the actual meshing situation of the gear tooth meshing area, considering the surface roughness, two points A (conjugate tooth root meshing point) and B (conjugate tooth top circle meshing point) are selected, and the analysis of contact load ratio W (roughness peak bearing load as a percentage of total load) and oil film thickness ratio λ (ratio of average oil film thickness to surface roughness) are performed under different working conditions. The analysis results shown in Fig. 9 and 10 were obtained. Fig. 9 shows the change curve of the contact load ratio and film thickness ratio of the points A and B with the rotation speed.
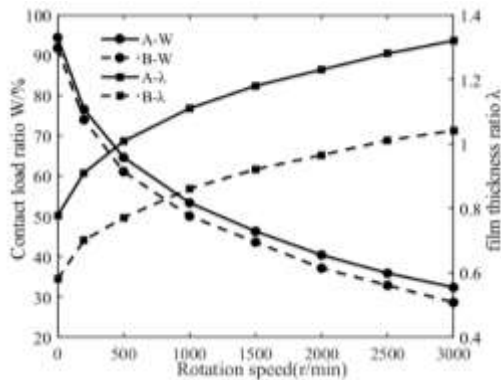
As can be seen from Fig. 9, when the rotation speed is less than 100 *rpm*, the load ratio W at each point is larger (more than 80%). When the speeds of points A and B are 300 *rpm* and 2500 *rpm*, respectively, the film thickness ratio λ is close to 1, and at this time, if the rotation speed continues to decrease, λ will be less than 1, and the lubrication effect will be poor. When the rotation speed increases, the contact load ratio W decrease, the film thickness ratio λ becomes larger, and the lubrication condition in the meshing area is improved. However, when the rotation speed is too large, the effect will gradually become smaller. At low speed, the film thickness is relatively small, and the rough peak contact between the contact surfaces increases. When the speed is too low, the film thickness ratio is less than 1, and the lubrication will turn to boundary lubrication, which will accelerate gear wear. Therefore, the harmonic reducer should appropriately increase the rotation speed to prevent poor lubrication.

In order to study the effect of temperature on the lubrication characteristics, without changing the speed and other factors, by changing the lubricant temperature, the analysis results are shown in Fig. 10.
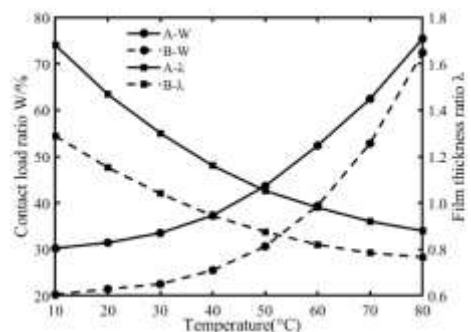

Fig. 10 *Effect of oil temperature on lubrication*

Fig. 9 *Effect of rotation speed on lubrication*

It can be seen from Fig. 8 that as the temperature increases, the contact load ratio

gradually increases and the film thickness ratio gradually decreases. This shows that the increase in temperature reduces the thickness of the lubricant film and increases the roughness peak load. And when the temperature at point *A* is greater than 60ºC and the temperature at point *B* is greater than 30ºC, the film thickness ratio will be less than 1, the oil film thickness will decrease, the lubrication will change from mixed lubrication to boundary lubrication, the rough peak contact between the contact surfaces will increase, and the lubrication effect will deteriorate. Therefore, avoiding long-term high temperature operation is conducive to improving the lubrication of harmonic gears and increasing gears life.

3.3 Effect of working conditions on the change of oil film stiffness

In order to further analyze the influence of working conditions on the oil film stiffness, the changes in oil film stiffness in the meshing area of the gear teeth along the direction of the meshing line under different rotation speed and oil temperature were calculated, as shown in Fig. 11.
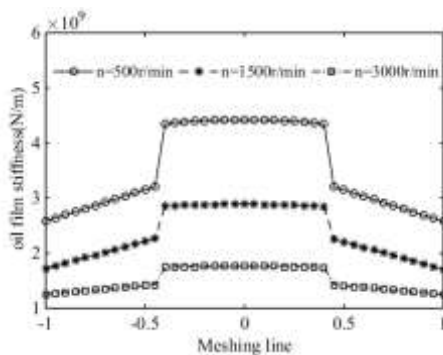
a)
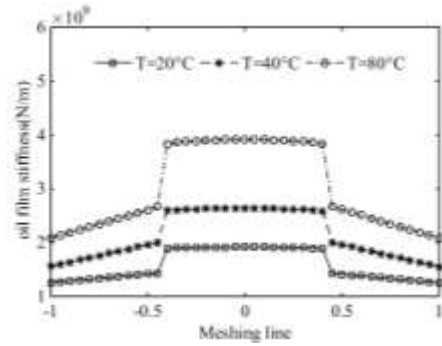
b)

Fig. 11 *Effect of working conditions on oil film stiffness; a)* effect of speed on oil film stiffness, and b) effect of temperature on oil film stiffness

It can be seen that the single-tooth meshing area of the oil film in the entrance area is relatively thin due to the large film thickness. However, the stiffness of the multi-tooth meshing region is greater due to the larger pressure peak, and sudden variation occurs at the alternate points of single-tooth and multi-teeth. As the speed increases, the stiffness of the oil film decreases significantly, and the sudden variation in stiffness gradually decrease. While the effect of temperature on stiffness is just the opposite: as the temperature increases, the oil film stiffness increases significantly, and the sudden variation in stiffness also becomes apparent. This shows that properly increasing the rotation speed and lowering the oil temperature can effectively reduce the oil film stiffness, thereby improving the overall stiffness of the gear teeth and reducing the system vibration.

4 Conclusion

For harmonic gear transmission, the parameters such as the integrated curvature radius, the entrainment velocity and the load at the meshing point of harmonic gear are analyzed and extracted, and the mathematical analysis model of

EHL of harmonic gear transmission based on the finite length line contact is established. Using the numerical calculation method to solve the model, the pressure and film thickness distribution in the lubrication area are obtained. The lubrication characteristic parameters such as the contact load ratio and film thickness ratio of the meshing points of the harmonic gear transmission under different rotational speeds and oil temperature conditions were analyzed, as well as the changes of the oil film stiffness. The results show that the pressure along the meshing direction reaches a peak at the center meshing point, the film thickness is larger in the entrance area, and it is evenly distributed in the center meshing area. Both the rotational speed and oil temperature have significant effect on the lubrication characteristics. Proper increase of the rotational speed can increase the film thickness ratio of meshing points and reduce the contact load ratio, which is beneficial to improving the lubrication characteristics of the meshing area and reducing the oil film stiffness. The influence of oil temperature on it is just the opposite. Increasing the temperature will reduce the film thickness ratio of the meshing point and reduce the contact load ratio, which will make the lubrication performance worse. Therefore, appropriately increasing the rotational speed and reducing the lubricant temperature can effectively improve the lubrication characteristics of the harmonic gear transmission system. The research results can provide a reference for the subsequent tooth wear failure mechanism of harmonic gear transmission and the development of nonlinear dynamic analysis.

5 ACKNOWLEDGEMENTS

6 NOMENCLATURES

C		the intersection of the line between the coordinate origin and the meshing point and the neutral line of the flexspline
E	[Pa]	equivalent modulus of elasticity
E_1, E_2	[Pa]	the elastic moduli of the flexspline and the circular spline materials, respectively
F	[N]	load between the flexspline and the circular spline
F_0	[N]	the maximum load
Δf	[Pa]	the load increase of the oil film
h	[m]	the oil film thickness
h_0	[m]	the central film thickness
$\Delta \bar{h}$	[m]	the average oil film thickness increase from the entrance area to the exit area
k		the meshing point
k_{oil}	[N/m]	the oil film stiffness
N		the parameter of the number of meshing teeth
n_1, n_2		the node numbers where the pressure in the inlet area is generated and the pressure in the outlet area disappears
O_{b1}, O_{b2}		the corresponding base circle

		centers of the flexspline and the circular spline, respectively
p	[Pa]	the oil film pressure
r_{b1}, r_{b2}	[m]	the base circle radii of the meshing point k on the flexspline and the circular spline, respectively
R	[m]	the comprehensive curvature radius at the meshing point
R_1	[m]	the distance from the center of the flexspline base circle to the meshing point
R_{k1}, R_{k2}	[m]	the curvature radii of meshing point of the flexspline and the circular spline, respectively
R, G		the tooth curves of the flexspline and the circular spline, respectively
T		the common normal line of the two base circles
T_0	[K]	the ambient temperature
T_1	[K]	the lubricant temperature
T_{in}	[N·m]	Torque
u	[ms^{-1}]	the entrainment velocity
V_K	[ms^{-1}]	the relative motion velocity of the k-point
V_{ek}	[ms^{-1}]	the velocity of the involved motion
V_{rk}	[ms^{-1}]	the velocity of the radial elastic deformation
V_{tk}	[ms^{-1}]	the velocity of the circumferential elastic deformation
W		the contact load ratio
v_1, v_2		the Poisson's ratios of the flexspline and the circular spline materials, respectively

ω	[rad/s]	the angular velocity
ω_H	[rad/s]	the angular velocity of the wave generator
ω_R	[rad/s]	the angular velocity of the flexspline
x		the direction of motion
y		the direction perpendicular to x
z		the number of the circular spline teeth
α		the viscosity pressure coefficient
β		the viscosity temperature coefficient
λ		oil film thickness ratio
ρ	[kg/m^3]	the lubricant density
ρ_0	[kg/m^3]	the environmental density
ρ_k	[m]	the polar radius of the meshing point k
η	[Ns/m^2]	the lubricant viscosity
η_0	[Ns/m^2]	environmental viscosity
$\mu(x, y)$	[μm]	the surface roughness
$\delta(x, y)$		the comprehensive elastic deformation
Ω		the calculation domain
φ		the position of meshing point
φ_m		the position of the maximum load
φ_0		the size of the actual meshing area

7 REFERENCES

[1] Tao, M., Chen, Y., Chen, D., Wu, J., Chen, F., Li, B., Mei, J. (2018). Research present status and outlook of harmonic reducer testing technology. *Journal of Mechanical Transmission*, vol. 42, no. 7, p. 175-180, **DOI: 10.16578/j.issn.1004.2539.2018.07.034.**

[2] Hu, Q., Liu, Z., Cai, L., Yang, C., Zhang, T., and Wang, G. (2019). Research on Prediction Method of Transmission Accuracy of Harmonic Drive. *International Design Engineering Technical Conferences and Computers and Information in Engineering Conference*, Vol. 59308, p. V010T11A006, **DOI：10.1115/DETC2019-97214.**

[3] Preumont P., Szewczyk R. (2018) Key Factors Influencing the Accuracy of Harmonic Gears for Space Applications. *Conference on Automation*. Springer, Cham, p. 483-489, **DOI：10.1007/978-3-319-77179-3_45**

[4] Concli, F. (2016). Windage, churning and pocketing power losses of gears: differentmodeling approaches for different goals. *Forschung im Ingenieurwesen*, vol. 80, no. 3-4, p. 85-99, **DOI：10.1007/s10010-016-0206-9.**

[5] Concli, F., Gorla, C. (2017). CFD simulation of power losses and lubricant flows in gearboxes. *American Gear Manufacturers Association Fall Technical Meeting*, p. 2-14.

[6] Concli, F., Gorla, C. (2016). Numerical modeling of the power losses in geared transmissions: Windage, churning and cavitation simulations with a new integrated approach that drastically reduces the computational effort. *Tribology International*, vol. 103. p. 58-68, **DOI: 10.1016/j.triboint.2016.06.046.**

[7] Jonson K. L. (1985). Contact mechanics. *London: Cambridge University Press*, p. 129-152.

[8] Wymer D. G., Cameron A. (1974). Elastohydrodynamic lubrication of a line contact. *Proc Instn Mech Engrs*, vol. 188, p. 221–238.

[9] Park T. J., Kim K. W. (1998). Elastohydrodynamic lubrication of a finite line contact. *Wear*, vol. 223, no. 1-2, p. 102-109. **DOI: 10.1016/S0043-1648(98)00317-2.**

[10] Zhu, C. C., Liu M. Y., Liu, H. J., Xu, X. Y., Liu, L. B. (2013). A thermal finite line contact EHL model of a helical gear pair. *Proceedings of the Institution of Mechanical Engineers, Part J: Journal of Engineering Tribology*, vol. 227, p. 299-309. **DOI: 10.1177/1350650112462324.**

[11] Wei, B., Wang, J., Zhou, G., Yang, R., Zhou, H., He, T. (2016) Mixed lubrication analysis of modified cycloidal gear used in the RV reducer. *Proceedings of the Institution of Mechanical Engineers, Part J: Journal of Engineering Tribology*, vol. 230, no. 2, p. 121-134, **DOI: 10.1177/1350650115593301.**

[12] Liu, H., Mao, K., Zhu, C., Chen, S., Xu, X., Liu, M. (2013) Spur gear lubrication analysis with dynamic loads. *Tribology Transactions*, vol. 56, no. 1, p. 41-48, **DOI: 10.1080/10402004.2012.725805.**

[13] Ouyang, T., Chen, N., Huang, J., Huang, H. (2016) Analysis of lubricating performance for spur gear pairs applying tribo-dynamic model. *Proceedings of the Institution of Mechanical Engineers, Part J: Journal of Engineering Tribology*, vol. 230, no. 10, p. 1244-1257, **DOI: 10.1177/1350650116631713.**

[14] Xiao, Z., Li, Z., Shi, X., Zhou, C. (2018) Oil film damping analysis in non-Newtonian transient thermal elastohydrodynamic lubrication for gear transmission. *Journal of Applied Mechanics*, vol. 85, no. 3, **DOI: 10.1115/1.4038697.**

[15] Sikorski, J., Pawlowski, W. (2020). Internal Friction of Ball Bearings at Very Low Temperatures. *Strojniski Vestnik-Journal of Mechanical Engineering*, vol. 66., no. 4, p. 235-242, **DOI: 10.5545/sv-jme.2019.6398.**

[16] Scaraggi, M. & De Novellis, L.,Carbone, G. (2010). EHL-Squeeze in Highly Loaded Contacts: The Case of Chain CVT Transmissions. *Strojniski Vestnik-Journal of Mechanical Engineering*, vol. 56, no. 4, p. 253-260.

[17] Ciulli, E., Bartilotta, I., Polacco, A., Manconi, S., Vela, D., Saverio, F., Paleotti, G. (2010). A Model for Scuffing Prediction. *Strojniski Vestnik-Journal of Mechanical Engineering*, vol. 56, no. 4, p. 231-238.

[18] Li, J., Chen, W., Zhang, L., Wang, T. (2016). An Improved Quasi-Dynamic Analytical Method to Predict Skidding in Roller Bearings under Conditions of Extremely Light Loads and Whirling. *Strojniski Vestnik-journal of Mechanical Engineering*, vol. 62, no. 2, p. 86-94. **DOI: 10.5545/sv-jme.2015.2848.**

[19] Li J., Wang J., Zhou G., Zheng J., Hao H. (2013) Study on failure mechanism of spatial lubrication harmonic reducer. *Tribology*, vol. 33, no. 1, p. 44-48, **DOI: 10.16078/j.tribology,.01.011.**

[20] Li, S. S., Shao, J., Yu, F., Ling, J., Chen, B. (2014). Research on modeling method for oil-film stiffness calculation of point contact based on EHL. *Advanced Materials Research. Trans Tech Publications*, vol. 945-949, p. 802-810, **DOI: 10.4028/www.scientific.net/amr.945-949.802.**